Thematic set:
The Mid-Carnian Episode

JGS
Journal of the Geological Society

Published Online First

https://doi.org/10.1144/jgs2017-170

Perturbations in the carbon cycle during the Carnian Humid Episode: carbonate carbon isotope records from southwestern China and northern Oman

Y.D. Sun[1]*, S. Richoz[2], L. Krystyn[3], Z.T. Zhang[4] & M.M. Joachimski[1]

[1] GeoZentrum Nordbayern, Universität Erlangen-Nürnberg, Schlossgarten 5, 91054 Erlangen, Germany
[2] Department of Geology, Lund University, Sölvegatan 12, Lund, Sweden
[3] Department of Palaeontology – Geozentrum, Althanstrasse 14, A-1090 Vienna, Austria
[4] College of Marine Science and Technology, China University of Geosciences (Wuhan), Wuhan 430074, P.R. China
Y.D.S., 0000-0003-4032-2082; S.R., 0000-0001-5424-3540
* Correspondence: yadong.sun@fau.de

Abstract: The Carnian Humid Episode is an interval of prominent climatic changes in the Late Triassic. We studied the carbon isotope ($\delta^{13}C$) geochemistry of carbonates from sections in southwestern China and northern Oman. $\delta^{13}C$ records from the Yongyue section (western Guizhou, South China) show a progressive positive shift from 1.4 to 2.8‰ in the early to middle Julian 1 substage. This positive trend is followed by a swift negative shift of *c.* 4.2‰ from 2.8 to −1.4‰ in the Julian 2 substage. $\delta^{13}C$ from the Wadi Mayhah section (northern Oman) shows a positive shift from 2.2 to 2.8‰ in the Julian 1 substage, followed by a negative shift of *c.* 3.2‰ from 2.8 to −0.3‰ in the Julian 2 substage. The $\delta^{13}C$ records from the two study sections generally correlate well with each other as well as with published records, pointing to a considerable input of isotopically light carbon starting in the late Julian 1 substage. Such a large amount of light carbon probably derived from direct degassing and the sediment–sill contact metamorphism of the Panthalassan Wrangellia Large Igneous Province and contemporary Tethyan volcanism. The voluminous volcanogenic greenhouse gases probably contributed to the warming pulse in the middle Carnian. Thus the dry–wet climatic transition during the Carnian Humid Episode is best interpreted as a warm climate-driven intensification of the activities of the atmospheric circulation and hydrological cycle.

Received 31 December 2017; **revised** 27 July 2018; **accepted** 9 August 2018

First introduced as the Carnian Pluvial Event by Simms & Ruffell (1989), the Carnian Humid Episode (CHE, following the latest term of Ruffell *et al.* 2015) represents an interval of major climatic changes in the Triassic Period, but remains the least understood. The CHE is characterized by a transient phase (<1 myr) of increased humidity in an otherwise long-lasting arid climate (Kozur & Bachmann 2010; Preto *et al.* 2010; Chatalov 2017; López-Gómez *et al.* 2017). The sudden climatic shift caused significant environmental and ecological changes, which are documented in both sedimentary and fossil records. On land, a clear shift in floral assemblages from xerophytes to hygrophytes is seen in the late Julian substage (Roghi *et al.* 2010; Mueller *et al.* 2016*a*, *b*), possibly promoting the changeovers in terrestrial tetrapods (Benton 1986, 1994; Bernardi *et al.* 2018). Peat-forming environments were steadily established in both North America and western Europe (Olsen 1988; Pott *et al.* 2008), representing their first occurrences in equatorial latitudes after the *c.* 15 myr coal gap from the end-Permian mass extinction (Retallack *et al.* 1996). In the oceans, the dry–wet climatic transition caused an increase in siliciclastic influx to the epicontinental seas (Stefani *et al.* 2010; Arche & López-Gómez 2014). Increased turbidity probably suppressed carbonate production, resulting in the demise of platforms and reef ecosystems in the western Tethys (Flügel & Senowbari-Daryan 2001; Hornung *et al.* 2007*a*; Preto *et al.* 2010). In the eastern Tethys (SW China), the CHE is manifested by the development of extensive oxygen-depleted facies on top of the fossiliferous platform and slope to basin carbonates (Sun *et al.* 2016). The deposition of black shales in the region was closely associated with anoxia and the development of local foreland basins on top of the former platform (Enos *et al.* 2006). Notable victims of the CHE in marine realms include platform and reef dwellers, such as encrinid crinoids, forams and scallops, as well as casualties in nektonic groups such as conodonts and ammonoids (Simms *et al.* 1994; Hornung *et al.* 2007*a*; Rigo *et al.* 2007; BouDagher-Fadel 2008; Chen *et al.* 2016). Losses on land are not yet fully quantified.

Perturbations in the carbon cycle often coincided with bio-crisis intervals in the geological past, mirroring significant environmental changes. The carbon isotope ratio ($\delta^{13}C$) of marine carbonates traces the carbon isotope composition of the dissolved inorganic carbon pool in the ocean and thus records a subtle equilibrium of carbon input (e.g. riverine carbon input and volcanic degassing) and carbon burial (e.g. carbonate and organic carbon) (Sharp 2017). Primary producers (i.e. phytoplankton and plants) preferentially utilize ^{12}C, synthesizing isotopically light organic matter. The organic matter rains down from the photic zone to the seafloor and might be either re-oxidized or buried with sediments (Hayes *et al.* 1999). Positive $\delta^{13}C$ excursions are generally interpreted as evidence for enhanced burial of organic carbon, either due to increases in primary productivity in the euphotic zone, oxygen deficiency in the water column, or both at the same time (Saltzman & Thomas 2012). Negative $\delta^{13}C$ excursions are caused by an increased input of isotopically light carbon from, for example, the remineralization of organic carbon, volcanism and contact metamorphism. As the CHE coincided with voluminous eruptions of the Wrangellia flood basalt, the negative $\delta^{13}C$ excursion during the CHE has been linked to the release of volcanogenic carbon (Dal Corso *et al.* 2012; Mueller *et al.* 2016*b*; Miller *et al.* 2017).

The carbonate production crisis and sudden siliciclastic fluxes during the CHE generated a carbonate gap in large areas in both western Tethys and the peri-Gondwana margins (Hornung *et al.*

2007*a*, *b*). Only a small number of $\delta^{13}C_{carb}$ studies have been carried out through (or partially through) the CHE interval (Keim *et al.* 2006; Hornung *et al.* 2007*b*; Dal Corso *et al.* 2015; Sun *et al.* 2016). Low total organic carbon contents and potential admixtures of terrestrial organic carbon in the siliciclastic rocks in different basins hinder the interpretation of $\delta^{13}C_{org}$ on the global scale (Dal Corso *et al.* 2015; Mueller *et al.* 2016*a*).

All sedimentary rocks are subject to diagenetic alteration. Thus sedimentary $\delta^{13}C$ records should be interpreted with prudence, especially in case of shallow water carbonates formed *in situ* on platforms. The original isotopic signatures can be substantially influenced by meteoritic diagenesis, a higher proportion of metastable aragonite relative to calcite and the local remineralization of organic matter (Patterson & Walter 1994; Immenhauser *et al.* 2003; Swart & Eberli 2005). Deeper water carbonates (e.g. slopes and ramps) are less prone to diagenetic overprinting and may preserve primary $\delta^{13}C_{carb}$ values, especially if they stabilized in a closed diagenetic system (Swart 2008). We carried out $\delta^{13}C_{carb}$ analyses on carbonates from a carbonate ramp setting in South China (the eastern Palaeotethys) and a periplatform deeper basin setting in Oman (the southern margin of the western Neotethys). The new data show a comparable negative shift in $\delta^{13}C_{carb}$ at the beginning of the CHE, pointing to an at least Tethyan-wide, if not global, disturbance in the global carbon cycle.

Geological setting

SW China is a classic location for Triassic studies as it has extensive outcrops of diverse sedimentary facies. Palaeomagnetic data suggest that SW China was situated in the Palaeotethys at *c.* 15° N in the Late Triassic (e.g. Wu *et al.* 1990). Palaeogeographically, SW China corresponds to the southwestern part of the Yangtze Platform and the Nanpanjiang Basin (Fig. 1). This platform and basin topography evolved into a foreland basin in the latest Carnian to Norian as a consequence of the Indosinian Orogeny (Enos *et al.* 1998; Sun *et al.* 2016). The study section at Yongyue (Guizhou Province, 25° 24′ 38.84″ N, 105° 33′ 23.07″ E) was located on the margin of the Yangtze Platform, documenting a continuous deepening from a carbonate platform setting in the Anisian to a basinal setting in the Carnian. The studied stratigraphic interval encompasses the Zhuganpo Formation and the lowermost part of the Wayao Formation (Fig. 2), spanning the earliest Julian 1 substage to the Julian 2 substage on the basis of conodont biostratigraphy (Zhang *et al.* 2017). The Zhuganpo Formation consists of a carbonate unit, whereas the Wayao Formation consists of black shales with rare carbonate beds. The transition of the two formations is marked by several condensed, ammonoid-bearing nodular limestone beds. Fossils from the Zhuganpo Formation are dominated by ammonoids, bivalves and crinoids. Rare fossils are seen in the Wayao Formation, except for ammonoid imprints, sponge spicules and *Halobia* bivalves, which occasionally occur in large numbers. Although they have a shorter stratigraphic range than the renowned sections in the Long Chang area (Enos *et al.* 1998; Sun *et al.* 2016), the strata at Yongyue are more expanded, allowing $\delta^{13}C_{carb}$ changes in the Julian substage to be seen at high resolution (Fig. 3).

Oman was situated at the southern passive continent margin of the western Neotethys and has a more complex geological history (e.g. Sengör 1984; Hauser *et al.* 2002). The Oman Mountains in the northeastern Arabian Peninsula (Fig. 1) are divided into five structural units: the 'Autochthonous' A and B; the Sumeini nappes (slope facies); the Hawasina nappes (basin facies); the Semail ophiolitic nappes; and the Neo-autochthonous platform deposits (Fig. 2; Glennie *et al.* 1974). Thin tectonic slices of the Hawasina nappes are squeezed between the Sumeini nappes and the Semail ophiolite, cropping out *c.* 700 km along the Oman Mountains (Bernoulli & Weissert 1987; Béchennec *et al.* 1990; Pillevuit *et al.* 1997; Maury *et al.* 2003; Wohlwend *et al.* 2017). The study section at Wadi Mayhah (24° 47′ 42.11″ N, 55° 53′ 50.39″ E) in northern Oman is situated *c.* 25 km west of the Emirati town of Hatta. Rocks cropped out in the section belong to the Hamrat Duru Group, which represents the lower tectonic units of the Hawasina nappes (Fig. 2).

The study succession consists of the upper part of the Al Jil Formation and the lower part of the Matbat Formation (following Béchennec *et al.* 1990 and corresponding to the Zulla Formation of Blechschmidt *et al.* 2004), generally representing a periplatform slope to basin setting (Immenhauser *et al.* 2000). The Al Jil Formation is characterized by a lower basalt unit of Ladinian age and an upper unit composed of alternations of shale, calci-turbidite and thin micritic limestone of early Carnian (Julian) age. The part of the Matbat Formation described here consists of green to dark brown radiolarian chert/cherty limestones with shales and calci-turbidites of late Carnian to early Norian age. The green cherts at the base of the Matbat Formation are dated in another section of the area (Sumeini, Wadi Shuab) to the middle Tuvalian (L. Krystyn, unpublished data). Thus the basal chert is either condensed or more probably represents a sedimentary hiatus at the boundary of the Al Jil and Matbat formations (Fig. 4). The absence of a sedimentary record of the Tuvalian 1 substage is a phenomenon known from other Tethyan pelagic carbonate sections. The overlying succession of calci-turbidite, chert and platy micritic limestone is dated to the Tuvalian 3–Lacian 1 (lower Norian) substages. Details of the biostratigraphic constraints are given in the Results section.

Methods

Both study sections were logged in detail and samples were collected at a comparable resolution. The Yongyue section was sampled at a resolution of *c.* 30–50 cm, yielding 107 samples. The Wadi Mayhah section was sampled at a resolution ranging from 20 to 60 cm, yielding 95 samples for $\delta^{13}C_{carb}$ and 10 samples for conodont biostratigraphy. For $\delta^{13}C_{carb}$ analyses, carbonate powders, preferably from micrites, were drilled on fresh-cut rock surfaces in the laboratory. The powders for the Yongyue section were reacted with 100% phosphoric acid at 70°C in a Gasbench II autosampler connected online to a ThermoFinnigan Delta V Plus mass spectrometer at GeoZentrum Nordbayern, University of Erlangen-Nuremberg (Germany). All values are reported as per mil relative to V-PDB by assigning $\delta^{13}C$ values of +1.95‰ to NBS19 and −47.3‰ to IAEA-CO9 and $\delta^{18}O$ values of −2.20‰ to NBS19 and −23.2‰ to NBS18. Reproducibility was monitored by replicate analysis of laboratory standards calibrated to NBS 19 and LSVEC and was ±0.08‰ for $\delta^{13}C_{carb}$ and ±0.05‰ for $\delta^{18}O_{carb}$ (1σ; $n = 19$). The powders for the Wadi Mayhah section were reacted with 100% phosphoric acid at 70°C for 3 min in a Kiel II autosampler. The resulting CO_2 was analysed with a Finnigan Delta Plus mass spectrometer at the Institute of Earth Sciences, Graz University (Austria). All values are reported as per mil relative to V-PDB by assigning $\delta^{13}C$ values of +1.95‰ to NBS19 and −5.01‰ to NBS18 and $\delta^{18}O$ values of −2.20‰ to NBS19 and −23.2‰ to NBS18. Reproducibility was monitored by replicate analysis of laboratory standards calibrated to NBS 19 and was ±0.06‰ for $\delta^{13}C_{carb}$ and ±0.08‰ for $\delta^{18}O_{carb}$ (1σ; $n = 24$). For conodont extraction, rocks were crushed into small chips and dissolved in formic acid at the Department of Palaeontology, University of Vienna (Austria).

Results

Biostratigraphy

At Yongyue, the nodular limestone beds at the top of the Zhuganpo Formation represent a very condensed interval and contain a well-

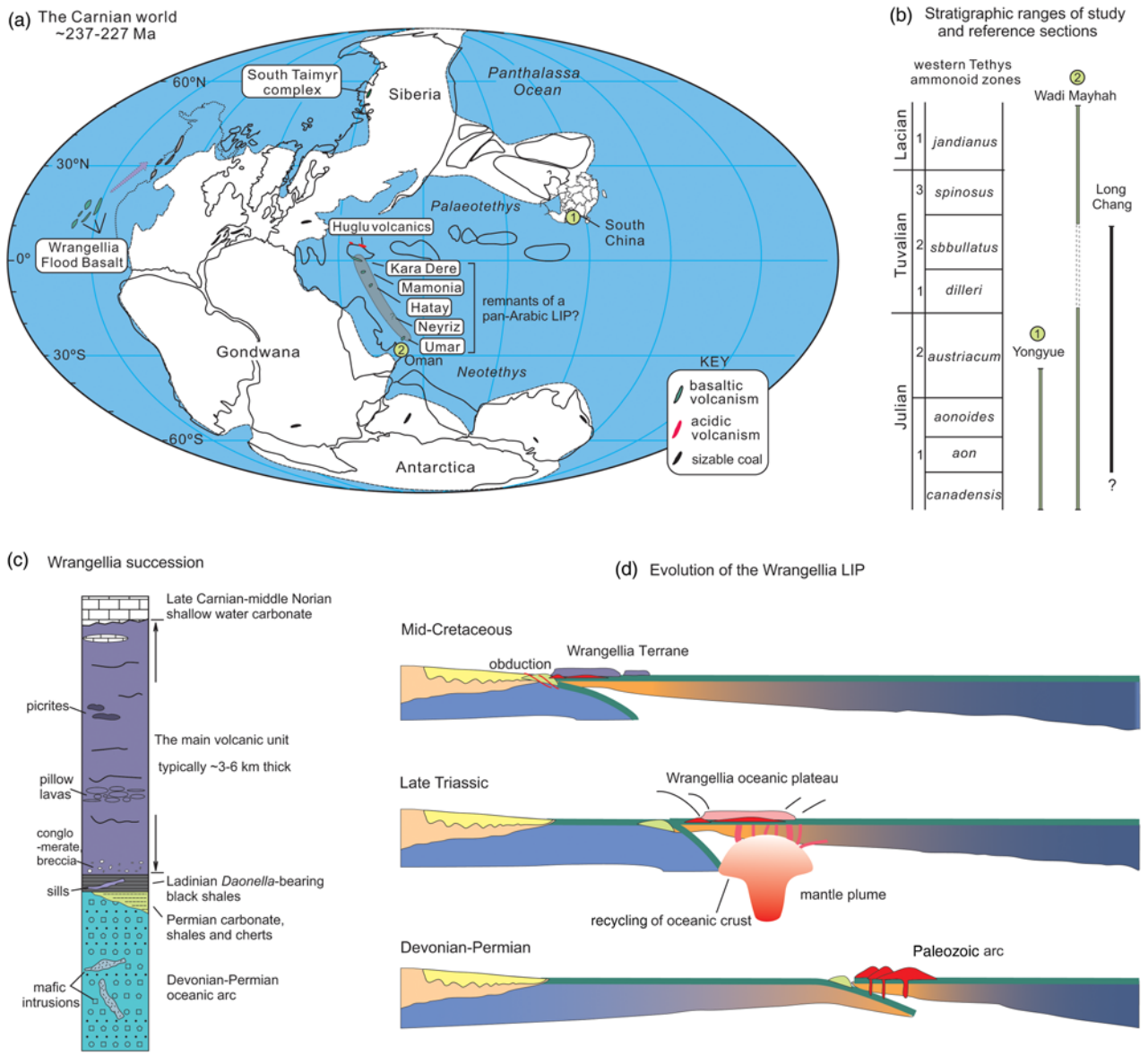

Fig. 1. (**a**) Palaeogeographical reconstruction of the Carnian world showing the locations of the study sections. Palaeomagnetic studies suggest that the Wrangellia LIP erupted at palaeolatitudes of 10–17° N (e.g. Hillhouse & Gromme 1984) and moved towards the NE until the middle Cretaceous. Sizeable coal measures are from Retallack *et al.* (1996). The Carnian volcanics are revised from Maury *et al.* (2008), Greene *et al.* (2010) and Sun *et al.* (2016). (**b**) Stratigraphic ranges of study and reference sections. (**c**) Simplified stratigraphy of the Wrangellia LIP, modified from Jones *et al.* (1977) and Greene *et al.* (2008, 2010). (**d**) Evolution of the Wrangellia Terrane based on references cited herein.

preserved ammonoid fauna. The ammonoids are in part endemic, bearing mixed features of *aonoides* and basal *austriacum* zones.

At Wadi Mayhah, the Al Jil Formation yields a typical Julian conodont fauna, consisting of *Budurovignathus*, *Paragondolella*, *Quadralella*, *Gladigondolella*, *Neovavitella* and *Mazzaella*. The Matbat Formation contains conodonts and bivalves of Tuvalian to Lacian age. *Carnepigondolella nodosa* is obtained at the 29 m level, suggesting a Tuvalian 3 age. At the 50 m level a thicker calci-turbidite bed contains a Lacian *Epigondolella quadrata* fauna. Coquina beds with bivalve *Halobia beyrichi* Mojsisovics are seen at the 53 m level and above, indicating a Lacian I/II age. Conodont ranges and images of Wadi Mayhah is shown in Figures 4 and 5, respectively.

Carbon isotopes

The $\delta^{13}C_{carb}$ values show similar patterns in the early Carnian part of the studied sections (Figs. 3 and 4). $\delta^{13}C_{carb}$ from Yongyue ranges from −1.4 to 2.8‰. It shows a steady increase from 1.4 to 2.8‰ in the Zhuganpo Formation. This is followed by a negative shift of 4.2‰, with $\delta^{13}C_{carb}$ values decreasing from 2.8‰ in the upper part of the Zhuganpo Formation to a minimum value of –1.4‰ in the lower Wayao Formation (Fig. 2). The transition from a positive shift to a negative shift in $\delta^{13}C_{carb}$ coincides with the development of thin black shales (*c.* 1–2 cm in thickness) interbedded between limestones in the upper Zhuganpo Formation. These appear more frequently with increasing thickness towards the Wayao Formation. Two concretion samples from the Wayao black shales were analysed to confirm that the $\delta^{13}C_{carb}$ values making up the curve are likely to be pristine and do not have a diagenetic overprint. Two $\delta^{13}C_{carb}$ data points are more negative, with more negative $\delta^{13}C_{carb}$ values (−5.5 and −4.3‰). $\delta^{13}C_{carb}$ and $\delta^{18}O_{carb}$ derived from the Yongyue samples do not systematically co-vary ($r = 0.08$; $P > 0.05$; $n = 107$; Fig. 6).

$\delta^{13}C_{carb}$ from Wadi Mayhah ranges from −0.3 to 3.7‰ and shows a minor increase from 2.2 to 2.7‰ in the lower part of the section. This is followed by a major negative excursion of 3.1‰ from 2.7 to −0.3‰ in the middle of the measured Al Jil Formation.

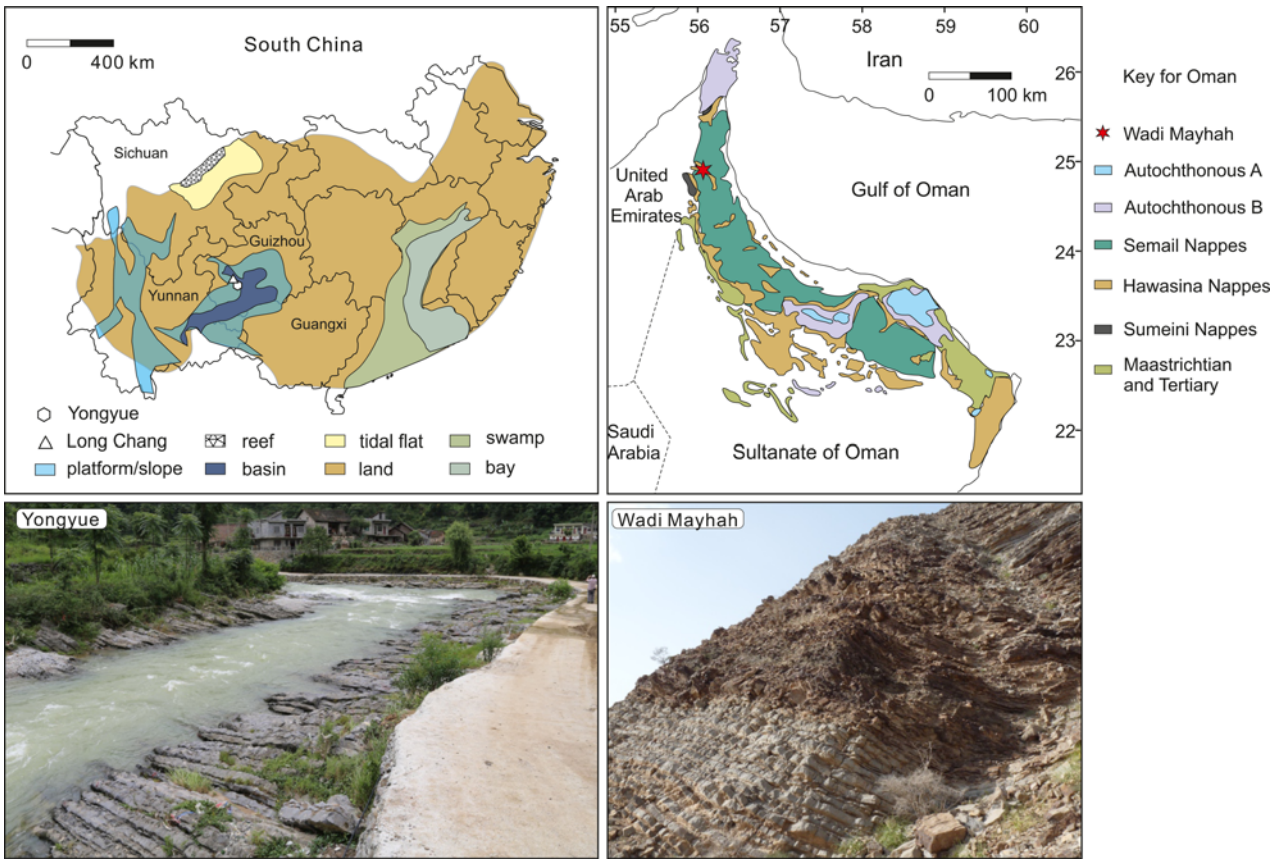

Fig. 2. Regional geology and field photography of the study sections. The regional palaeogeographical reconstructions of South China and Oman are modified from Ma *et al.* (2009) and Glennie *et al.* (1974), respectively. The field photograph of the Yongyue section shows the Zhuganpo limestone cropping out along the river bed. The field photograph of Wadi Mayhah shows the transition from the grey limestones of the uppermost Al Jil Formation to the dark brown and green chert of the Matbat Formation.

This overall negative shift is characterized by several minor positive and negative excursions, with amplitudes typically <1‰. A recovery phase of the negative excursion is registered in the uppermost Al Jil Formation, where $\delta^{13}C_{carb}$ values increase to 3.7‰. The $\delta^{13}C_{carb}$ data from the Matbat Formation show minor oscillations between 2.1 and 3.2‰, with minima at the *c.* 38 m level (Fig. 4). $\delta^{13}C_{carb}$ and $\delta^{18}O_{carb}$ do not significantly co-vary ($r = 0.15$; $P > 0.05$; $n = 95$, Fig. 6).

Discussion

Changes in sedimentation during the CHE

Changes in sedimentation are registered in study sections at the Julian 1–Julian 2 boundary, coinciding with the main phase of the CHE. The sedimentation rates are distinctly different in the studied sections. The strata at Wadi Mayhah are generally thinner. The Julian 1 substage at Wadi Mayhah is *c.* 10 m thick, whereas the Julian 1 substage at Yongyue is *c.* 60 m thick. However, at Wadi Mayhah, the Julian 2 is more expanded. The Julian 1–2 transition is marked by a change from cherty carbonate sedimentation to a more detrital carbonate–shale combination. Common occurrences of shale and calci-turbidite suggest regular sediment input from a nearby carbonatic–terrigeneous shelf. The cherty carbonate sedimentation resumed up-section after a hiatus, starting from the Tuvalian 2 substage (Fig. 4). At Yongyue, the Julian 1–Julian 2 transition is marked by the development of nodular limestone boundary beds at the top of the Zhuganpo Formation. This interval represents a highly condensed level. The onset of black shale sedimentation is immediately above this level, documenting an intensive anoxic event developed in the Nanpanjiang Basin (Sun *et al.* 2016).

Perturbations in the carbon cycle in the Carnian

The $\delta^{13}C_{carb}$ data from Yongyue show a clearly increasing trend in the early to middle Julian 1 substage, followed by a sharp decrease from the late Julian 1 to the Julian 2 substage. The $\delta^{13}C_{carb}$ trend is, in general, consistent with that from the nearby Long Chang section (Sun *et al.* 2016), showing minor spatial variations in the same basin (Fig. 7). Because $\delta^{13}C_{carb}$ and $\delta^{18}O_{carb}$ are not related, whereas the $\delta^{13}C_{carb}$ trend is regionally reproducible, the $\delta^{13}C_{carb}$ record from Yongyue is likely to be primary. However, we do not interpret the topmost two data points from the Wayao Formation. The two values are very negative and the carbonate concretions from which they were derived were probably products of early diagenesis. In examples with high organic matter and low carbonate contents, as seen in the Wayao Formation, the remineralization of organic matter in pore waters probably contributed to carbonate (re-)precipitation, leading to more negative $\delta^{13}C_{carb}$ values, as seen in our concretion samples. Thus the ^{13}C depleted signature might have resulted from exchanges of carbon with the surrounding organic-rich black shales.

The $\delta^{13}C_{carb}$ record from Wadi Mayhah generally correlates well with the South China records, with only some minor discrepancies. The decrease in $\delta^{13}C_{carb}$ in the Julian substage consists of two shifts: an initial decrease in $\delta^{13}C_{carb}$ from *c.* 3.0 to 2.0‰ (shift 1) and a main sharp decrease in $\delta^{13}C_{carb}$ from *c.* 2.0 to 0‰ (shift 2) (Fig. 7). However, the Tuvalian $\delta^{13}C_{carb}$ from Oman is not directly correlatable with the Long Chang record from South China due to a major sedimentary gap in the lower Tuvalian, a phenomenon seen in almost all Oman Hawasina nappe sections. In addition, the predominantly cherty sedimentation in the lower Matbat Formation (middle Tuvalian) hampered sampling for both carbon isotopes and conodonts.

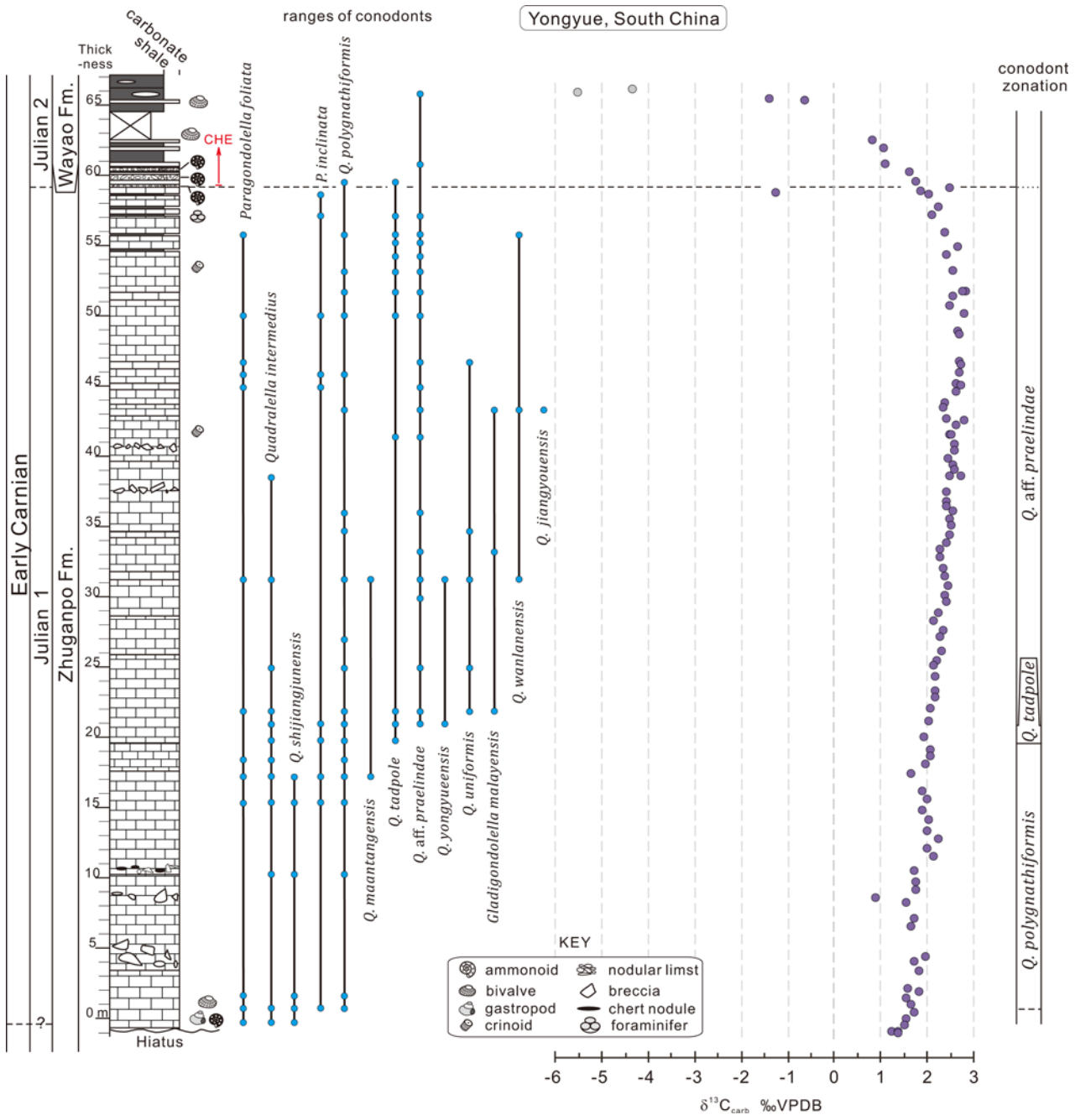

Fig. 3. Log of the Yongyue section (South China) with $\delta^{13}C_{carb}$ data (this study) and conodont ranges (from Zhang *et al.* 2017).

Both the Zhuganpo and Al Jil formations are bioturbated and fossiliferous, suggesting stable and constantly well-oxygenated environments. The progressive increase in $\delta^{13}C_{carb}$ seen in the lower Zhuganpo Formation and the 0 to 4 m level of the Al Jil Formation is also registered in the $\delta^{13}C_{org}$ in the Northern Calcareous Alps and the Transdanubian Range (Dal Corso *et al.* 2015), suggesting that this positive trend is probably a global signature. The trend was probably caused by the enhanced burial of organic matter, possibly due to an increase in primary productivity in the ocean and/or the accumulation of coal on land in the early and middle Julian 1 substage.

The significant negative excursions in $\delta^{13}C_{carb}$ starting in the late Julian 1 substage can be explained by (1) the input of isotopically light carbon by combined volcanic outgassing of the Wrangellia oceanic plateau and contemporaneous Tethyan volcanic activities (Maury *et al.* 2008; Greene *et al.* 2010; Dal Corso *et al.* 2012) and (2) a sharp decrease in primary productivity and/or reduced burial of organic matter. Both processes could enrich ^{12}C in the oceanic dissolved inorganic carbon pool and result in a negative shift in $\delta^{13}C_{carb}$. Evidence supporting scenario 2 is by far insubstantial. The CHE represents only a secondary bio-crisis and major decreases in primary productivity (or extinctions of primary producers) have not been reported. Instead, the burial of light carbon increased both in the ocean and on land.

Oceanic anoxia was widespread from the Julian 2 substage, as documented in the extensive deposition of black shales and organic-rich marls in several Tethyan basins and along peri-Gondwana margins (Bellanca *et al.* 1995; Keim *et al.* 2006; Hornung *et al.* 2007*b*; Soua 2014; Sun *et al.* 2016). The renewed occurrence of sizeable coal seams occurred globally in the Carnian (Retallack *et al.* 1996). The most notable coal accumulation is the bituminous coal of mid-Carnian age from the Newark rift system basins in North America. More than 10 million tons were mined from the eighteenth century to the beginning of the twentieth century, with an estimated *c.* 4 billion tons remaining (Robbins *et al.* 1988). The widespread

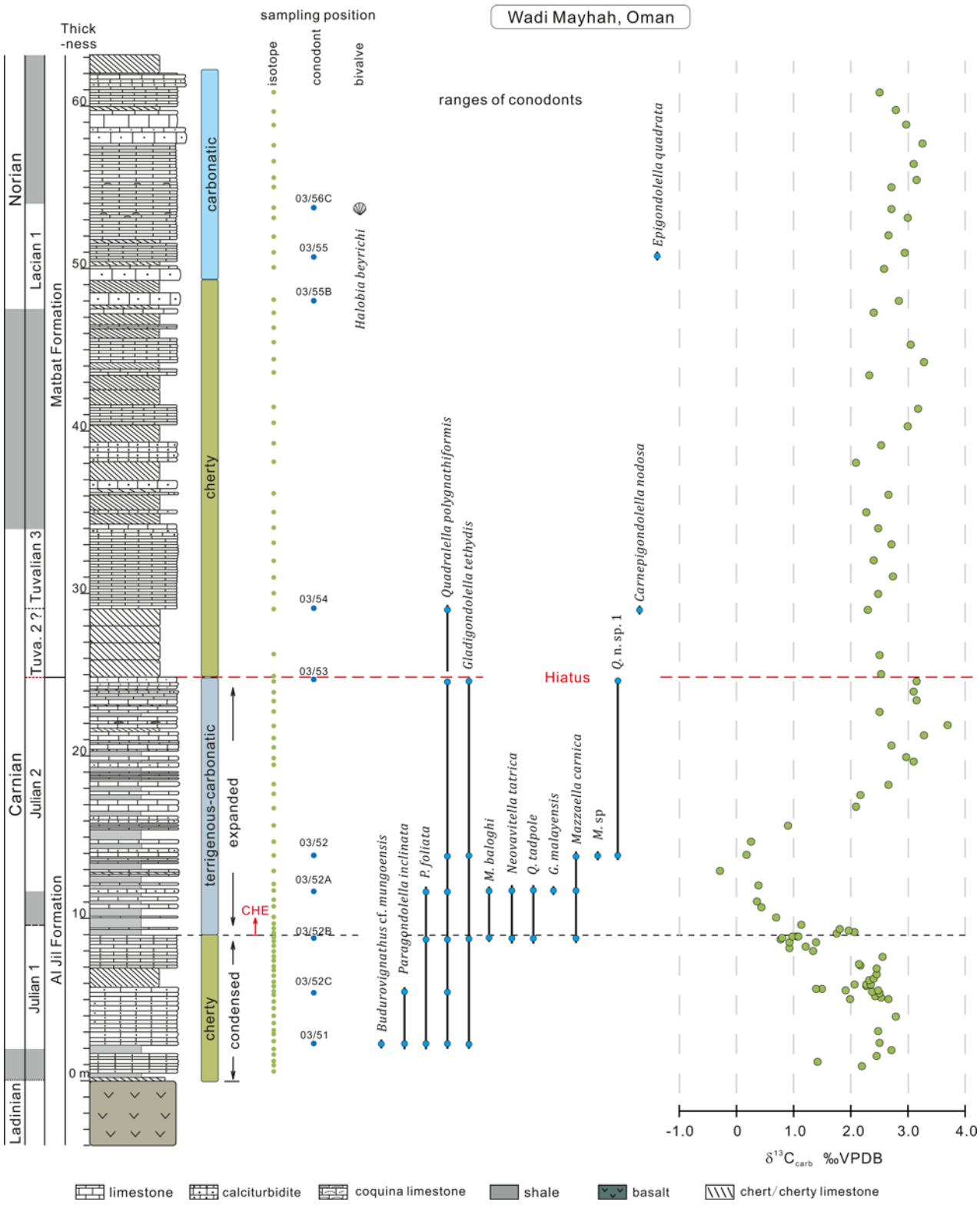

Fig. 4. Log of the Wadi Mayhah section (Oman) with $\delta^{13}C_{carb}$ data and conodont ranges. Note the change from cherty carbonate to more siliciclastic sedimentations occurred at the Julian 1-Julian 2 transition.

burial of coal may have further contributed to the fixation of organic matter on land and should result in a positive shift in $\delta^{13}C_{carb}$ depending on the amount of organic carbon being stored. Many of the coals in the Newark Supergroup are of Julian age (Olsen 1990). The large negative excursion of *c.* 3–4‰ seen during the CHE requires a substantial input of isotopically light carbon to compensate for the enhanced burial of organic carbon, both on land and in the oceans.

A tectonically induced CHE v. a volcanically induced CHE

The driving mechanism of the CHE is a matter of intense debate. Conventional theories suggest the mega-monsoonal climate induced by the supercontinent configuration or changes in the local oceanography as potential causes (Simms & Ruffell 1990; Kozur & Bachmann 2010; Rigo *et al.* 2012). Sedimentary evidence suggests that the monsoonal climate reached maximum strength in the Triassic (Parrish 1993), leading to more arid conditions in the

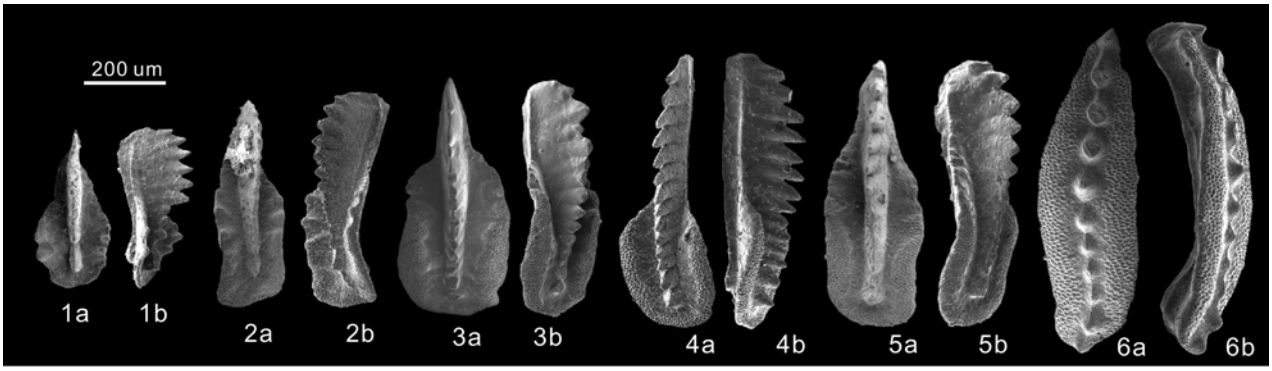

Fig. 5. Scanning electron microscopy images of conodonts (selected) from Wadi Mayhah, Oman. 1, *Mazzaella baloghi* (Kovács 1977), 03-52A-34; 2, *Mazzaella carnica* (Tollmann & Krystyn 1975), 03-52A-32; 3, *Mazzaella* sp. 03-52-08; 4, *Quadralella tadpole* (Hayashi 1968), 03-52A-30; 5, *Quadralella polygnathiformis* (Budurov & Stefanov 1965), 03-52A-36; 6, *Gladigondolella malayensis* Nogami 1968, 03-52A-27. Parts 'a' are the upper view and parts 'b' are the lateral view.

Pangaean intervals and more humid conditions with stronger seasonality around coastal areas (Tanner 2018). However, it has been argued that tectonically induced environmental changes are generally long-lasting, contradicting the transient nature of the CHE (Sun *et al.* 2016; Miller *et al.* 2017), whereas strong seasonality may be too short to be recorded in the sedimentary record. Negative carbon isotope excursions, such as that seen in South China and Oman during the CHE, require major inputs of light carbon into the global carbon cycle. Tectonics are unlikely to have had a significant role in such short-lived perturbations of the carbon cycle. Kozur & Bachmann (2010) instead postulated that the closure of the Palaeotethys opened a southern seaway, cutting through the western Cimmerian microcontinent and resulting in an influx of warm water into the NW Tethyan basins. It was further suggested that the increase in seawater temperatures in NW Tethys (Hornung *et al.* 2007*a*) could have changed the regional climate, leading to wetter conditions. However, the western European basins were situated in low latitudes at *c.* 10–20° N during the Carnian. An increase in seawater temperatures of >4°C caused by heat exchange with slightly more southerly waters (shown in fig. 5 of Kozur & Bachmann 2010) over *c.* 1 myr seems unlikely. An increase in seawater temperatures of a comparable amplitude is also registered in the eastern Tethys, suggesting a global, rather than regional, warming event (Sun *et al.* 2016). The hypothesis of Kozur & Bachmann (2010) should thus be rejected. Instead, our $\delta^{13}C_{carb}$ data support a hypothesis that warming during the CHE was induced by increased atmospheric pCO_2 levels.

Large Igneous Provinces and carbon cycle instability

Eruptions of Large Igneous Provinces (LIPs) coincide with many mass extinctions and lesser calamities in the geological past (Wignall 2001; Courtillot & Renne 2003; Bond & Wignall 2014; Bond & Grasby 2017). LIP activities are characterized by voluminous outflows of lavas (typically of the order of 10^6 km^3), accompanied by the injection of enormous amounts of volatiles into the atmosphere over a short time interval (<5 myr; Ernst & Youbi 2017). As volcanogenic and thermogenic CO_2 and CH_4 are isotopically light and act as competent greenhouse gases, the degassing of LIPs often causes both negative $\delta^{13}C$ excursions and global warming, best exemplified by the eruptions of the Siberian Traps during the Permian–Triassic transition (Svensen *et al.* 2009; Joachimski *et al.* 2012; Sun *et al.* 2012). The Wrangellia LIP might have played a similar part during the CHE (Dal Corso *et al.* 2012), although the negative $\delta^{13}C$ excursion of *c.* 3–4‰ seen during the CHE is smaller than the *c.* 4–7‰ excursion seen during the end-Permian mass extinction (Korte & Kozur 2010).

The Greater Wrangellia Terrane (Fig. 1) is part of the North American Cordilleran and reaches from Idaho, along the western coast of Canada, to southern Alaska, representing an obducted oceanic plateau on top of a Paleozoic oceanic arc (Coney & Jones 1985). Palaeomagnetic studies suggest that the Wrangellia LIP erupted at equatorial latitudes around 10–17° N and moved northeastwards to its current position in the middle Cretaceous (Hillhouse & Gromme 1984). The Wrangellia basaltic succession, typically *c.* 3.5–6 km thick, overlies the middle Ladinian *Daonella*-bearing black shales and underlies upper Carnian to middle Norian platform and reefal carbonates (Jones *et al.* 1977; Stanley 1989). Thus the timing of the eruptions is biostratigraphically constrained to an interval between the late Ladinian and the early Carnian, with local eruptions possibly still occurring in the Norian. A sharp decrease in the $^{187}Os/^{188}Os$ ratio in the late Ladinian is interpreted to be due to an increase in mantle-derived ^{187}Os from Wrangellia volcanism (Xu *et al.* 2014).

The environmental impacts of the Wrangellia eruptions are not yet fully evaluated. The estimated maximum volume of the Wrangellia LIP is only 0.14×10^6 km^3, about half of the Middle Permian Emeishan LIP and about 3.5 to 14 % of the Permian–

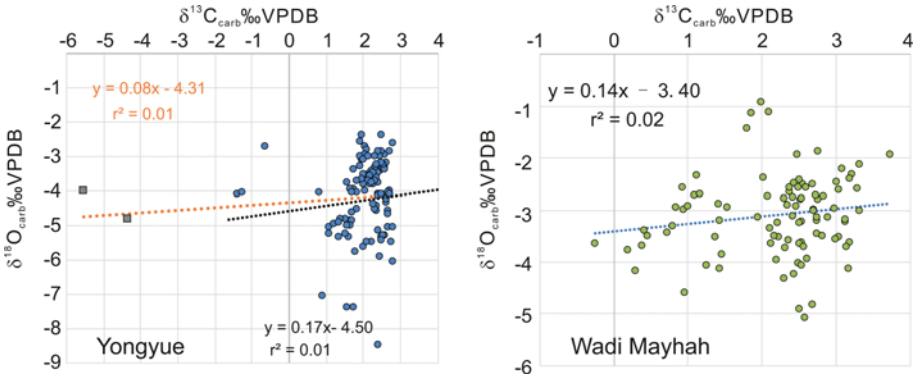

Fig. 6. Cross-plot of $\delta^{13}C_{carb}$ and $\delta^{18}O_{carb}$ showing the low correlation coefficient in both study sections. The two data points from concretions in the Yongyue section (square symbols) are grey in colour. The black trend line represents the linear regression in which the two outliers are excluded.

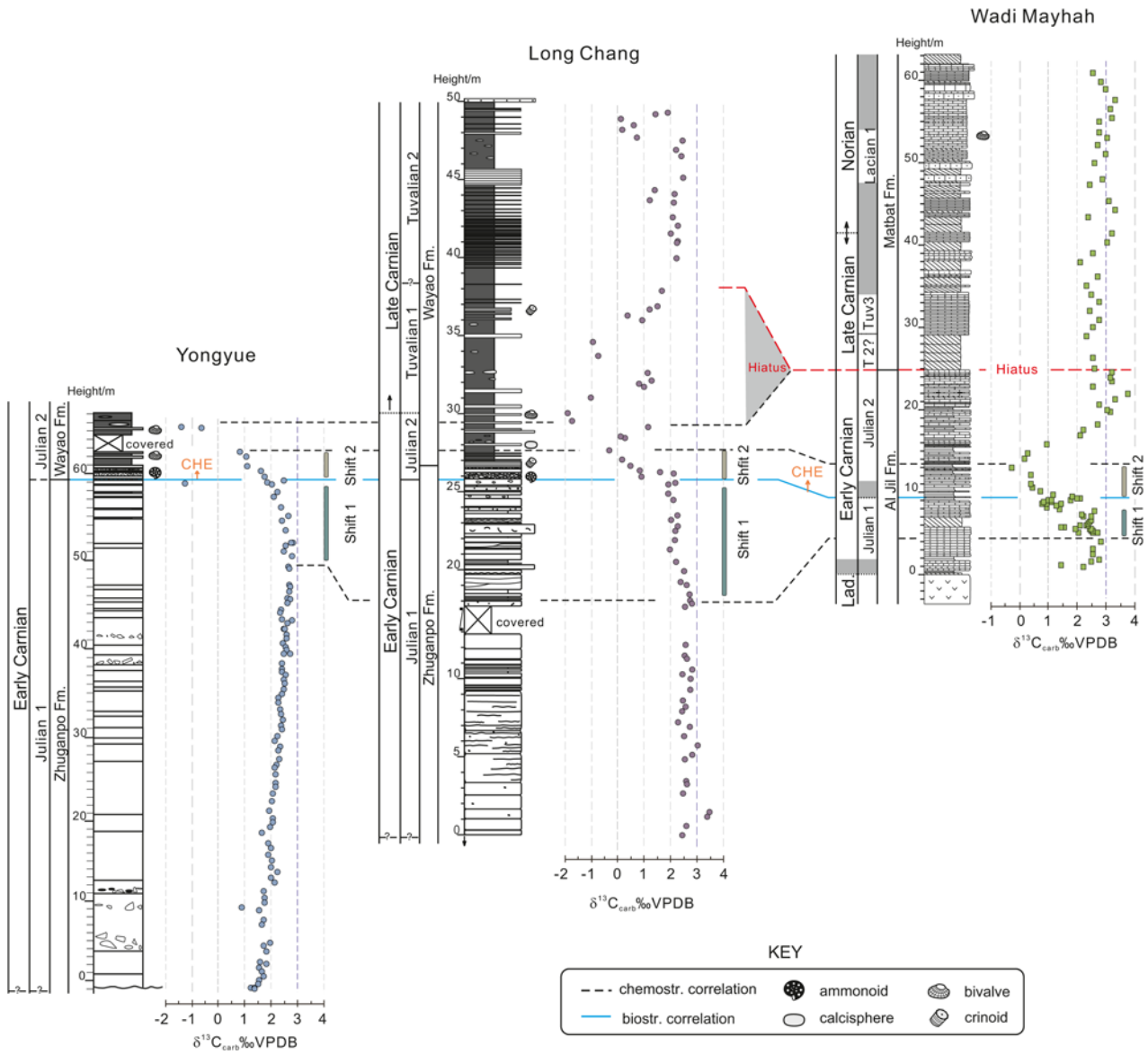

Fig. 7. Correlation of $\delta^{13}C_{carb}$ records from Yongyue and Long Chang, SW China and Wadi Mayhah, northern Oman. Data from Long Chang are from Sun *et al.* (2016).

Triassic Siberian Traps (Courtillot *et al.* 1999; Ali *et al.* 2005; Greene *et al.* 2010). It is arguable whether a small LIP such as the Wrangellia could trigger large environmental perturbations to a crisis level (e.g. Tanner 2018). Indeed, volcanogenic CO_2 is not very ^{13}C-depleted ($\delta^{13}C = -5‰$) (Saltzman & Thomas 2012). Hence other mechanisms should be invoked for a small LIP triggering a large $\delta^{13}C$ excursion and serious global climatic impacts. The Wrangellia LIP shares many similarities with its Middle Permian counterpart. Both LIPs overlie sedimentary rocks, were erupted at equatorial latitudes, developed many sills and dykes, and had phases of phreatomagmatic eruptions (Hillhouse & Gromme 1984; Wignall *et al.* 2009; Sun *et al.* 2010). Eruptions in these settings are much more violent and are able to inject volatiles more easily to the stratosphere and therefore influence the global climate.

Picrite from the Wrangellia succession indicates a melting temperature of *c.* 1500°C, supporting a mantle plume origin for the LIP (Greene *et al.* 2009). The LIP developed on top of a Paleozoic oceanic arc (Jones *et al.* 1977; Greene *et al.* 2008). The subducted oceanic crust and pre-existing arc lithosphere were inevitably recycled in the head of the plume (Fig. 1c). Under such conditions, massive amounts of CO_2 and HCl were probably released from recycled oceanic crust and alone could have triggered a mass extinction event (Sobolev *et al.* 2011). In addition to direct outgassing from lavas, contact metamorphism can release further greenhouse gases. Volatile production (typically CH_4, CO_2, SO_2, H_2O and halogens) by a single sill can last for 10–1000 years. If there is contact with organic-rich shales (i.e. TOC > 5 wt%, in this case the *Donella*-bearing black shales), thermogenic CH_4 can be produced and released at a rate of 85–135 g m^{-3} (Retallack & Jahren 2008; Aarnes *et al.* 2010; Stordal *et al.* 2017). If there is contact with carbonates (in this case the Golden Horn Limestone), the reaction dolomite = periclase + calcite + CO_2 occurs, producing 240 g of CO_2 per kg of dolomite (Ganino & Arndt 2009). The thick sediment–sill complex developed on Vancouver Island and in the Alaska Range (Greene *et al.* 2008; 2009) suggests that such contact metamorphic processes probably occurred across large areas of the Wrangellia LIP. It is important to note that the activities of several coeval Tethyan volcanic events (e.g. the Huglu and Kara Dere traps) may have played key parts in contributing additional carbon to compensate for the small volume of the Wrangellian LIP, allowing environmental impacts of green-house gas release to cross the critical threshold for the start of the CHE at the Julian 1–2 boundary.

Other contemporaneous volcanism in the Carnian

The Carnian was a time of intense volcanic activity. In addition to the Wrangellia LIP, several other volcanic centres were active, probably contributing additional carbon inputs to the atmosphere. These include both basaltic and silicic volcanism in Huglu-Pindos and Kara Dere (Turkey), Mamonia (Cyprus) and South Taimyr (Russia) (Fig. 1). As only minor relicts of these volcanic complexes are preserved, the environmental effects induced by their eruptions remain challenging to differentiate and evaluate. Both the Kara Dere Basalt and Mamonia Complex are probably remnants of Late Triassic oceanic crust and sea plateaus, possibly of the same origin (Maury *et al.* 2008). The Kara Dere type basalt is also seen as the lower Carnian base of Oman intra-oceanic exotics (e.g. the Haliw sequence and J. Khawr shallow water carbonates) (Blendinger 1991). It is difficult to estimate their original sizes due to the strong tectonic overprinting associated with the opening of the Neotethys when the Semail Ophiolite of Oman (Fig. 2) was emplaced onto the Arabian continental margin as a result of northeastwards subduction in the Late Cretaceous (Searle & Cox 1999). It is possible that the early Carnian intra-ocean opening of Gondwana (Arabia) was widespread from Greece to Turkey, Iran(?), Oman and beyond, forming a large Pan-Arabic LIP in which large volumes of volcanics were built up, but almost all the remnants have been subducted or eroded after obduction (for reconstructions, see Fig. 1a). The Kara Dere type basalts show no sign of crustal contamination (i.e. igneous rocks of crust affinity) in their components, but contain recycled marine sediments (Lapierre *et al.* 2007; Maury *et al.* 2008). The recycling of sediments, especially carbonates, in magma chambers probably has similar effects to contact metamorphism, releasing extra volatiles (e.g. Lee *et al.* 2012).

Carbon input, warming and the CHE

Massive emissions of volcanogenic gases into the atmosphere result in potent greenhouse effects, driving the global climate to a warmer state. Higher temperatures enhance evaporation (thus increasing water saturation in the atmosphere) and increase temperature differences on both the land and in the oceans. An intensified atmospheric circulation and hydrological cycle could culminate in the transition from dry to wet conditions during the CHE. Climate warming may initiate water column stratification and the deoxygenation of deeper waters, leading to enhanced carbon burial at the seafloor. Warm and wet climatic conditions amplify both the bacterial and fungal decomposition of organic matter and the chemical weathering of silicates on land. The former releases CO_2, thus exerting a positive feedback on the warm climate, whereas the latter consumes CO_2, exerting a negative feedback on the elevated atmospheric pCO_2 (Brady 1991). Thus the climatic conditions of the Carnian evolved in a precarious balance of positive and negative feedbacks of the initial carbon release. Though a slow-acting process, the intense chemical weathering of continental crust, together with the enhanced burial of organic carbon in the ocean, may have counteracted the warming effects of greenhouse gas emissions and driven the climatic conditions to a steady state, ultimately terminating the CHE.

Conclusions

The carbon isotope composition of carbonates from the Yongyue section (China) in the eastern Palaeotethys and the Wadi Mayhah section (Oman) in the southern Neotethys have been measured. Although the study sections were situated in different palaeogeographical settings, both show generally consistent patterns of $\delta^{13}C_{carb}$. The comparable negative $\delta^{13}C_{carb}$ excursion suggests that the instability of the carbon cycle during the CHE was Tethyan-wide and most likely a global phenomenon. The input of isotopically light carbon can be related to volcanic degassing and thermogenic heating of organic-rich sediments as a consequence of the Wrangellia LIP and other contemporary volcanic activities. The dry–wet transition during the CHE thus coincided with a large input of carbon into the atmosphere and a shift in sedimentation from (cherty) carbonates to shales in study areas, and was most probably due to the intensification of the hydrological cycle triggered by volcanism-induced global warming.

Acknowledgements This is a contribution to Deutsche Forschungsgemeinschaft (DFG, German Science Foundation) Research Unit TERSANE (FOR 2332: Temperature-related stressors as a unifying principle in ancient extinctions; Project Jo 219/15). S.R. and L.K. conducted fieldwork in Oman under authorization of the Public Authority for Mining, Sultanate of Oman. The authors thank D. Lutz and L.N. Wang for laboratory and field assistance. Comments from Editor J. Dal Corso and two reviewers significantly improved this paper.

Funding The National Key R&D Program of China (grant no. 2016YFA0601100), National Natural Science Foundation of China (grant no. 41602026, 41821001) financially supported this study. S.R. and L. K. were sponsored by the Austrian National Committee for IGCP (IGCP630).

Correction notice: Some minor spelling mistakes as well as the spelling of L. Krystyn has been corrected following a submission error.

Scientific editing by Jacopo Dal Corso

References

Aarnes, I., Svensen, H., Connolly, J.A.D. & Podladchikov, Y.Y. 2010. How contact metamorphism can trigger global climate changes: modeling gas generation around igneous sills in sedimentary basins. *Geochimica et Cosmochimica Acta*, **74**, 7179–7195, https://doi.org/10.1016/j.gca.2010.09.011

Ali, J.R., Thompson, G.M., Zhou, M.F. & Song, X.Y. 2005. Emeishan large igneous province, SW China. *Lithos*, **79**, 475–489, https://doi.org/10.1016/j.lithos.2004.09.013

Arche, A. & López-Gómez, J. 2014. The Carnian Pluvial Event in Western Europe: new data from Iberia and correlation with the Western Neotethys and Eastern North America–NW Africa regions. *Earth-Science Reviews*, **128**, 196–231, https://doi.org/10.1016/j.earscirev.2013.10.012

Béchennec, F., Le Metour, J., Rabu, D., Bourdillon-de-Grissac, C., de Wever, P., Beurrier, M. & Villey, M. 1990. The Hawasina Nappes: stratigraphy, palaeogeography and structural evolution of a fragment of the south-Tethyan passive continental margin. *In*: Robertson, A.H.F., Searle, M.P. & Ries, A.C. (eds) *The Geology and Tectonics of the Oman Region*. *Geological Society, London, Special Publications*, **49**, 213–223, https://doi.org/10.1144/gsl.sp.1992.049.01.14

Bellanca, A., Di Stefano, P. & Neri, R. 1995. Sedimentology and isotope geochemistry of Carnian deep-water marl/limestone deposits from the Sicani Mountains, Sicily: environmental implications and evidence for a planktonic source of lime mud. *Palaeogeography, Palaeoclimatology, Palaeoecology*, **114**, 111–129, https://doi.org/10.1016/0031-0182(95)00077-Y

Benton, M.J. 1986. More than one event in the late Triassic mass extinction. *Nature*, **321**, 857–861, https://doi.org/10.1038/321857a0

Benton, M.J. 1994. Late Triassic to Middle Jurassic extinctions among continental tetrapods: testing the pattern. *In*: Fraser, N.C. & Sues, H.-D. (eds) *In the Shadow of the Dinosaurs*. Cambridge University Press, Cambridge, 366–397.

Bernardi, M., Gianolla, P., Petti, F.M., Mietto, P. & Benton, M.J. 2018. Dinosaur diversification linked with the Carnian Pluvial Episode. *Nature Communications*, **9**, 1499, https://doi.org/10.1038/s41467-018-03996-1

Bernoulli, D. & Weissert, H. 1987. The upper Hawasina nappes in the central Oman Mountains: stratigraphy, palinspastics and sequence of nappe emplacement. *Geodinamica Acta*, **1**, 47–58, https://doi.org/10.1080/09853111.1987.11105124

Blechschmidt, I., Dumitrica, P., Matter, A., Krystyn, L. & Peters, T. 2004. Stratigraphic architecture of the northern Oman continental margin – Mesozoic Hamrat Duru Group Hawasina complex, Oman. *Geo-Arabia*, **9**, 81–132.

Blendinger, W. 1991. Al Aridh Formation, Oman: stratigraphy and palaeogeographic significance. *In:* Peters, T., Nicolas, A. & Coleman, R.G. (eds) *Ophiolite Genesis and Evolution of the Oceanic Lithosphere: Proceedings of the Ophiolite Conference, held in Muscat, Oman, 7–18 January 1990*. Springer, Dordrecht, 575–592.

Bond, D.P.G. & Grasby, S.E. 2017. On the causes of mass extinctions. *Palaeogeography, Palaeoclimatology, Palaeoecology*, **478**, 3–29, https://doi.org/10.1016/j.palaeo.2016.11.005

Bond, D.P.G. & Wignall, P.B. 2014. Large igneous provinces and mass extinctions: an update. *In*: Keller, G. & Kerr, A.C. (eds) *Volcanism, Impacts, and Mass Extinctions: Causes and Effects*. *Geological Society of America, Special Papers*, **505**, https://doi.org/10.1130/2014.2505(02)

BouDagher-Fadel, M.K. 2008. *Evolution and Geological Significance of Larger Benthic Foraminifera. Developments in Palaeontology & Stratigraphy, 21*. Elsevier Science, Amsterdam.

Brady, P.V. 1991. The effect of silicate weathering on global temperature and atmospheric CO_2. *Journal of Geophysical Research: Solid Earth*, **96**, 18101–18106, https://doi.org/10.1029/91JB01898

Chatalov, A. 2017. Quartz arenites and laterites in the Moesian Group (Upper Triassic), northwestern Bulgaria: possible evidence for the effect of the Carnian Humid Episode. *Geologica Balcanica*, **46**, 3–25.

Chen, Y., Krystyn, L., Orchard, M.J., Lai, X.-L. & Richoz, S. 2016. A review of the evolution, biostratigraphy, provincialism and diversity of Middle and early Late Triassic conodonts. *Papers in Palaeontology*, **2**, 235–263, https://doi.org/10.1002/spp2.1038

Coney, P.J. & Jones, D.L. 1985. Accretion tectonics and crustal structure in Alaska. *Tectonophysics*, **119**, 265–283, https://doi.org/10.1016/0040-1951(85)90042-3

Courtillot, V. & Renne, P. 2003. On the ages of flood basalt events. *Comptes Rendus Academie des sciences. Geoscience*, **335**, 113–140, https://doi.org/10.1016/S1631-0713(03)00006-3

Courtillot, V., Jaupart, C., Manighetti, I., Tapponnier, P. & Besse, J. 1999. On causal links between flood basalts and continental breakup. *Earth and Planetary Science Letters*, **166**, 177–195, https://doi.org/10.1016/S0012-821X(98)00282-9

Dal Corso, J., Mietto, P., Newton, R.J., Pancost, R.D., Preto, N., Roghi, G. & Wignall, P.B. 2012. Discovery of a major negative $\delta^{13}C$ spike in the Carnian (Late Triassic) linked to the eruption of Wrangellia flood basalts. *Geology*, **40**, 79–82, https://doi.org/10.1130/g32473.1

Dal Corso, J., Gianolla, P. *et al.* 2015. Carbon isotope records reveal synchronicity between carbon cycle perturbation and the 'Carnian Pluvial Event' in the Tethys realm (Late Triassic). *Global and Planetary Change*, **127**, 79–90, https://doi.org/10.1016/j.gloplacha.2015.01.013

Enos, P., Wei, J. & Lehrmann, D.J. 1998. Death in Guizhou — Late Triassic drowning of the Yangtze carbonate platform. *Sedimentary Geology*, **118**, 55–76, https://doi.org/10.1016/s0037-0738(98)00005-0

Enos, P., Lehrmann, D.J. *et al.* 2006. *Triassic Evolution of the Yangtze Platform in Guizhou Province, People's Republic of China.* Geological Society of America, Special Papers, **417**, 1–105, https://doi.org/10.1130/2006.2417

Ernst, R.E. & Youbi, N. 2017. How large igneous provinces affect global climate, sometimes cause mass extinctions, and represent natural markers in the geological record. *Palaeogeography, Palaeoclimatology, Palaeoecology*, **478**, 30–52, https://doi.org/10.1016/j.palaeo.2017.03.014

Flügel, E. & Senowbari-Daryan, B. 2001. Triassic reefs of the Tethys. *In*: Stanley, G.D. (ed.) *The History and Sedimentology of Ancient Reef Systems*. Springer, Boston, MA, 217–249.

Ganino, C. & Arndt, N.T. 2009. Climate changes caused by degassing of sediments during the emplacement of large igneous provinces. *Geology*, **37**, 323–326, https://doi.org/10.1130/g25325a.1

Glennie, K.W., Boeuf, M.G.A., Hughes Clarke, M.W., Moody-Stuart, M., Pilaar, W.F. & Reinhardt, B.M. 1974. Geology of the Oman Mountains. *Verhandelingen van her Koninklijk Nederlands geologisch mijnbouwkundig Genootschap*, **31**, 1–423.

Greene, A.R., Scoates, J.S. & Weis, D. 2008. Wrangellia flood basalts in Alaska: a record of plume–lithosphere interaction in a Late Triassic accreted oceanic plateau. *Geochemistry, Geophysics, Geosystems*, **9**, Q12004, https://doi.org/10.1029/2008GC002092

Greene, A.R., Scoates, J.S., Weis, D., Nixon, G.T. & Kieffer, B. 2009. Melting history and magmatic evolution of basalts and picrites from the accreted Wrangellia Oceanic Plateau, Vancouver Island, Canada. *Journal of Petrology*, **50**, 467–505, https://doi.org/10.1093/petrology/egp008

Greene, A.R., Scoates, J.S., Weis, D., Katvala, E.C., Israel, S. & Nixon, G.T. 2010. The architecture of oceanic plateaus revealed by the volcanic stratigraphy of the accreted Wrangellia oceanic plateau. *Geosphere*, **6**, 47–73, https://doi.org/10.1130/ges00212.1

Hauser, M., Martini, R., Matter, A., Krystyn, L., Peters, T., Stampfli, G. & Zaninetti, L. 2002. The break-up of East Gondwana along the northeast coast of Oman: evidence from the Batain basin. *Geological Magazine*, **139**, 145–157, https://doi.org/10.1017/S0016756801006264

Hayes, J.M., Strauss, H. & Kaufman, A.J. 1999. The abundance of ^{13}C in marine organic matter and isotopic fractionation in the globlal biogeochemical cycle of carbon during the past 800 Ma. *Chemical Geology*, **161**, 103–125, https://doi.org/10.1016/S0009-2541(99)00083-2

Hillhouse, J.W. & Gromme, C.S. 1984. Northward displacement and accretion of Wrangellia: new paleomagnetic evidence from Alaska. *Journal of Geophysical Research: Solid Earth*, **89**, 4461–4477, https://doi.org/10.1029/JB089iB06p04461

Hornung, T., Brandner, R., Krystyn, L., Joachimskimo, M.M. & Keim, L. 2007*a*. Multistratigraphic constraints on the NW Tethyan 'Carnian Crisis'. *In*: Lucas, S.G. and Spielmann, J.A. (eds) *The Global Triassic. New Mexico Museum of Natural Histroy and Science Bulletin*, **41**, 59–67.

Hornung, T., Krystyn, L. & Brandner, R. 2007*b*. A Tethys-wide mid-Carnian (Upper Triassic) carbonate productivity crisis: evidence for the Alpine Reingraben event from Spiti (Indian Himalaya)? *Journal of Asian Earth Sciences*, **30**, 285–302, https://doi.org/10.1016/j.jseaes.2006.10.001

Immenhauser, A., Schreurs, G., Gnos, E., Oterdoom, H.W. & Hartmann, B. 2000. Late Palaeozoic to Neogene geodynamic evolution of the northeastern Oman margin. *Geological Magazine*, **137**, 1–18, https://doi.org/10.1017/S0016756800003526

Immenhauser, A., Della Porta, G., Kenter, J.A.M. & Bahamonde, J.R. 2003. An alternative model for positive shifts in shallow-marine carbonate $\delta^{13}C$ and $\delta^{18}O$. *Sedimentology*, **50**, 953–959, https://doi.org/10.1046/j.1365-3091.2003.00590.x

Joachimski, M.M., Lai, X. *et al.* 2012. Climate warming in the latest Permian and the Permian–Triassic mass extinction. *Geology*, **40**, 195–198, https://doi.org/10.1130/G32707.1

Jones, D.L., Silberling, N.J. & Hillhouse, J. 1977. Wrangellia—a displaced terrane in northwestern North America. *Canadian Journal of Earth Sciences*, **14**, 2565–2577, https://doi.org/10.1139/e77-222

Keim, L., Spöti, C. & Brandner, R. 2006. The aftermath of the Carnian carbonate platform demise: a basinal perspective (Dolomites, southern Alps). *Sedimentology*, **53**, 361–386, https://doi.org/10.1111/j.1365-3091.2006.00768.x

Korte, C. & Kozur, H.W. 2010. Carbon-isotope stratigraphy across the Permian–Triassic boundary: a review. *Journal of Asian Earth Sciences*, **39**, 215–235, https://doi.org/10.1016/j.jseaes.2010.01.005

Kozur, H.W. & Bachmann, G.H. 2010. The Middle Carnian wet intermezzo of the Stuttgart Formation (Schilfsandstein), Germanic Basin. *Palaeogeography, Palaeoclimatology, Palaeoecology*, **290**, 107–119, https://doi.org/10.1016/j.palaeo.2009.11.004

Lapierre, H., Bosch, D., Narros, A., Mascle, G.H., Tardy, M. & Demant, A. 2007. The Mamonia Complex (SW Cyprus) revisited: remnant of Late Triassic intra-oceanic volcanism along the Tethyan southwestern passive margin. *Geological Magazine*, **144**, 1–19, https://doi.org/10.1017/S0016756806002937

Lee, C.T.A., Shen, B. *et al.* 2012. Continental arc-island arc fluctuations, growth of crustal carbonates, and long-term climate change. *Geosphere*, **9**, 21–36, https://doi.org/10.1130/ges00822.1

López-Gómez, J., Escudero-Mozo, M.J., Martín-Chivelet, J., Arche, A., Lago, M. & Galé, C. 2017. Western Tethys continental–marine responses to the Carnian Humid Episode: palaeoclimatic and palaeogeographic implications. *Global and Planetary Change*, **148**, 79–95, https://doi.org/10.1016/j.gloplacha.2016.11.016

Ma, Y.S., Chen, D.H. & Wang, G.L. 2009. *Atlas of Tectonics, Sediments, Sequences and Lithofacies Palaeogeography from Sinian to Paleogene Periods in Southern China*. Science Press, Beijing.

Maury, R.C., Béchennec, F., Cotten, J., Caroff, M., Cordey, F. & Marcoux, J. 2003. Middle Permian plume-related magmatism of the Hawasina Nappes and the Arabian Platform: implications on the evolution of the Neotethyan margin in Oman. *Tectonics*, **22**, 1073, https://doi.org/10.1029/2002TC001483

Maury, R.C., Lapierre, H. *et al.* 2008. The alkaline intraplate volcanism of the Antalya nappes (Turkey): a Late Triassic remnant of the Neotethys. *Bulletin de la Societe geologique de France*, **179**, 397–410, https://doi.org/10.2113/gssgfbull.179.4.397

Miller, C.S., Peterse, F., da Silva, A.-C., Baranyi, V., Reichart, G.J. & Kürschner, W.M. 2017. Astronomical age constraints and extinction mechanisms of the Late Triassic Carnian crisis. *Scientific Reports*, **7**, 2557, https://doi.org/10.1038/s41598-017-02817-7

Mueller, S., Hounslow, M.W. & Kürschner, W.M. 2016*a*. Integrated stratigraphy and palaeoclimate history of the Carnian Pluvial Event in the Boreal realm; new data from the Upper Triassic Kapp Toscana Group in central Spitsbergen (Norway). *Journal of the Geological Society*, **173**, 186–202, https://doi.org/10.1144/jgs2015-028

Mueller, S., Krystyn, L. & Kürschner, W.M. 2016*b*. Climate variability during the Carnian Pluvial Phase — a quantitative palynological study of the Carnian sedimentary succession at Lunz am See, Northern Calcareous Alps, Austria. *Palaeogeography, Palaeoclimatology, Palaeoecology*, **441**, 198–211, https://doi.org/10.1016/j.palaeo.2015.06.008

Olsen, P.E. 1988. Paleontology and paleoecology of the Newark Supergroup (early Mesozoic, eastern North America). *In*: Manspeizer, W. (ed.) *Triassic–Jurassic Rifting and the Opening of the Atlantic Ocean*. Elsevier, Amsterdam, 185–230.

Olsen, P.E. 1990. Tectonic, climatic, and biotic modulation of lacustrine ecosystems – examples from Newark Supergroup of Eastern North America. *In*: Katz, B.J. (ed.) *Lacustrine Basin Exploration: Case Studies and Modern Analogs. AAPG Memoirs*, **50**, 209–224.

Parrish, J.T. 1993. Climate of the supercontinent Pangea. *Journal of Geology*, **101**, 215–233, https://doi.org/10.1086/648217

Patterson, W.P. & Walter, L.M. 1994. Depletion of $\delta^{13}C$ in seawater ΣCO_2, on modern carbonate platforms: significance for the carbon isotopic record of carbonates. *Geology*, **22**, 885–888, https://doi.org/10.1130/0091-7613(1994)022<0885:DOCISC>2.3.CO;2

Pillevuit, A., Marcoux, J., Stampfli, G. & Baud, A. 1997. The Oman Exotics: a key to the understanding of the Neotethyan geodynamic evolution. *Geodinamica Acta*, **10**, 209–238, https://doi.org/10.1080/09853111.1997.11105303

Pott, C., Krings, M. & Kerp, H. 2008. The Carnian (Late Triassic) flora from Lunz in Lower Austria: paleoecological considerations. *Palaeoworld*, **17**, 172–182, https://doi.org/10.1016/j.palwor.2008.03.001

Preto, N., Kustatscher, E. & Wignall, P.B. 2010. Triassic climates – state of the art and perspectives. *Palaeogeography, Palaeoclimatology, Palaeoecology*, **290**, 1–10, https://doi.org/10.1016/j.palaeo.2010.03.015

Retallack, G.J. & Jahren, H.A. 2008. Methane release from igneous intrusion of coal during Late Permian extinction events. *Journal of Geology*, **116**, 1–20, https://doi.org/10.1086/524120

Retallack, G.J., Veevers, J.J. & Morante, R. 1996. Global coal gap between Permian–Triassic extinction and Middle Triassic recovery of peat-forming plants. *Geological Society of America Bulletin*, **108**, 195–207, https://doi.org/10.1130/0016-7606(1996)108<0195:GCGBPT>2.3.CO;2

Rigo, M., Preto, N., Roghi, G., Tateo, F. & Mietto, P. 2007. A rise in the carbonate compensation depth of western Tethys in the Carnian (Late Triassic): deep-water evidence for the Carnian Pluvial Event. *Palaeogeography, Palaeoclimatology, Palaeoecology*, **246**, 188–205, https://doi.org/10.1016/j.palaeo.2006.09.013

Rigo, M., Trotter, J.A., Preto, N. & Williams, I.S. 2012. Oxygen isotopic evidence for Late Triassic monsoonal upwelling in the northwestern Tethys. *Geology*, **40**, 515–518, https://doi.org/10.1130/g32792.1

Robbins, E.I., Wilkes, G.P. & Textoris, D.A. 1988. Chapter 27 – Coal deposits of the Newark rift system. *In*: Manspeizer, W. (ed.) *Triassic–Jurassic Rifting. Continental Breakup and the Origin of the Atlantic Ocean and Passive Margins*. Developments in Geotectonics. Elsevier, 649–682.

Roghi, G., Gianolla, P., Minarelli, L., Pilati, C. & Preto, N. 2010. Palynological correlation of Carnian humid pulses throughout western Tethys. *Palaeogeography, Palaeoclimatology, Palaeoecology*, **290**, 89–106, https://doi.org/10.1016/j.palaeo.2009.11.006

Ruffell, A., Simms, M.J. & Wignall, P.B. 2015. The Carnian Humid Episode of the late Triassic: a review. *Geological Magazine*, **153**, 271–284, https://doi.org/10.1017/s0016756815000424

Saltzman, M.R. & Thomas, E. 2012. Carbon isotope stratigraphy. *In*: Gradstein, F.M., Ogg, J.G., Schmitz, M. & Ogg, G. (eds) *The Geologic Time Scale 2012*. Elsevier, Boston, 207–232.

Searle, M. & Cox, J. 1999. Tectonic setting, origin, and obduction of the Oman ophiolite. *Geological Society of America Bulletin*, **111**, 104–122, https://doi.org/10.1130/0016-7606(1999)111<0104:TSOAOO>2.3.CO;2

Sengör, A.M.C. 1984. *The Cimmeride Orogenic System and the Tectonics of Eurasia*. Geological Society of America Special Papers, **195**, 1–82, https://doi.org/10.1130/SPE195-p1

Sharp, Z. 2017. *Principles of Stable Isotope Geochemistry*. 2nd edn, https://doi.org/10.5072/FK2GB24S9F

Simms, M.J. & Ruffell, A.H. 1989. Synchroneity of climatic change and extinctions in the Late Triassic. *Geology*, **17**, 265–268, https://doi.org/10.1130/0091-7613(1989)017<0265:soccae>2.3.co;2

Simms, M.J. & Ruffell, A.H. 1990. Climatic and biotic change in the late Triassic. *Journal of the Geological Society*, **147**, 321–327, https://doi.org/10.1144/gsjgs.147.2.0321

Simms, M.J., Ruffell, A.H. & Johnson, A.L.A. 1994. Biotic and climatic changes in the Carnian (Triassic) of Europe and adjacent areas. *In*: Fraser, N.C. & Sues, H. (eds) *In the Shadow of the Dinosaurs: Early Mesozoic Tetrapods*. Cambridge University Press, New York, 352–365.

Sobolev, S.V., Sobolev, A.V. *et al.* 2011. Linking mantle plumes, large igneous provinces and environmental catastrophes. *Nature*, **477**, 312–316, https://doi.org/10.1038/nature10385

Soua, M. 2014. Early Carnian anoxic event as recorded in the southern Tethyan margin, Tunisia: an overview. *International Geology Review*, **56**, 1884–1905, https://doi.org/10.1080/00206814.2014.967315

Stanley, G.D. 1989. An Upper Triassic Reefal Limestone, Southern Vancouver Island, B.C. *In*: Geldsetzer, H.H.J., James, N.P. & Tebbutt, G.E. (eds) *Reef: Canada and Adjacent Areas*. Canadian Society of Petroleum Geologists, Memoirs, **13**, 766–775.

Stefani, M., Furin, S. & Gianolla, P. 2010. The changing climate framework and depositional dynamics of Triassic carbonate platforms from the Dolomites. *Palaeogeography, Palaeoclimatology, Palaeoecology*, **290**, 43–57, https://doi.org/10.1016/j.palaeo.2010.02.018

Stordal, F., Svensen, H.H., Aarnes, I. & Roscher, M. 2017. Global temperature response to century-scale degassing from the Siberian Traps large igneous province. *Palaeogeography, Palaeoclimatology, Palaeoecology*, **471**, 96–107, https://doi.org/10.1016/j.palaeo.2017.01.045

Sun, Y.D., Lai, X.L. *et al.* 2010. Dating the onset and nature of the Middle Permian Emeishan large igneous province eruptions in SW China using conodont biostratigraphy and its bearing on mantle plume uplift models. *Lithos*, **119**, 20–33, https://doi.org/10.1016/j.lithos.2010.05.012

Sun, Y.D., Joachimski, M.M. *et al.* 2012. Lethally hot temperatures during the Early Triassic greenhouse. *Science*, **338**, 366–370, https://doi.org/10.1126/science.1224126

Sun, Y.D., Wignall, P.B. *et al.* 2016. Climate warming, euxinia and carbon isotope perturbations during the Carnian (Triassic) Crisis in South China. *Earth and Planetary Science Letters*, **444**, 88–100, https://doi.org/10.1016/j.epsl.2016.03.037

Svensen, H., Planke, S., Polozov, A.G., Schmidbauer, N., Corfu, F., Podladchikov, Y.Y. & Jamtveit, B. 2009. Siberian gas venting and the end-Permian environmental crisis. *Earth and Planetary Science Letters*, **277**, 490–500, https://doi.org/10.1016/j.epsl.2008.11.015

Swart, P.K. 2008. Global synchronous changes in the carbon isotopic composition of carbonate sediments unrelated to changes in the global carbon cycle. *Proceedings of the National Academy of Sciences of the United States of America*, **105**, 13741–13745, https://doi.org/10.1073/pnas.0802841105

Swart, P.K. & Eberli, G. 2005. The nature of the $\delta^{13}C$ of periplatform sediments: implications for stratigraphy and the global carbon cycle. *Sedimentary Geology*, **175**, 115–129, https://doi.org/10.1016/j.sedgeo.2004.12.029

Tanner, L.H. 2018. Climates of the Late Triassic: perspectives, proxies and problems. *In*: Tanner, L.H. (ed) *The Late Triassic World: Earth in a Time of Transition*. Springer International, Cham, 59–90.

Wignall, P.B. 2001. Large igneous provinces and mass extinctions. *Earth-Science Reviews*, **53**, 1–33, https://doi.org/10.1016/S0012-8252(00)00037-4

Wignall, P.B., Sun, Y.D. *et al.* 2009. Volcanism, mass extinction, and carbon isotope fluctuations in the Middle Permian of China. *Science*, **324**, 1179–1182, https://doi.org/10.1126/science.1171956

Wohlwend, S., Celestino, R., Reháková, D., Huck, S. & Weissert, H. 2017. Late Jurassic to Cretaceous evolution of the eastern Tethyan Hawasina Basin (Oman Mountains). *Sedimentology*, **64**, 87–110, https://doi.org/10.1111/sed.12326

Wu, H.N., Liu, C., Chang, C. & Zhong, D. 1990. Evolution of the Qinling fold belt and the movement of the North and South China Blocks: the evidence of geology and paleomagnetism. *Scientia Geologica Sinica*, **3**, 201–214.

Xu, G., Hannah, J.L. *et al.* 2014. Cause of Upper Triassic climate crisis revealed by Re–Os geochemistry of Boreal black shales. *Palaeogeography, Palaeoclimatology, Palaeoecology*, **395**, 222–232, https://doi.org/10.1016/j.palaeo.2013.12.027

Zhang, Z.T., Sun, Y.D., Lai, X.L., Joachimski, M.M. & Wignall, P.B. 2017. Early Carnian conodont fauna at Yongyue, Zhenfeng area and its implication for Ladinian–Carnian subdivision in Guizhou, South China. *Palaeogeography, Palaeoclimatology, Palaeoecology*, **486**, 142–157, https://doi.org/10.1016/j.palaeo.2017.02.011